Internet Journal of Society for Social Management Systems Vol.12 Issue 1 sms19-3671
ISSN: 2432-552X
ORIGINAL ARTICLE

Numerical Simulation of Rupture Protrusion of Vertically Tightened PC Steel Bars Using Applied Element Method

Addisu Desalegne Bonger[1]*, Akira Hosoda[2], Hamed Salem[3], Kazuya Kaba[4]

[1] Graduate School of Urban Innovation, Yokohama National University, 79-5 Tokiwadai, Hodogaya-ku, Yokohama 240-8501 JAPAN

[2] Professor, Institute of Urban Innovation, Yokohama National University, 79-5 Tokiwadai, Hodogaya-ku, Yokohama 240-8501 JAPAN

[3] Professor, Structural Engineering Department, Cairo University, Jamaa Street, Giza 12316, EGYPT

[4] Mr. Kaba Kazuya, Capital Highway Co., Ltd., Maintenance Technology Division, 1-4-1 Kasumigaseki Chiyoda-ku, Tokyo 100-8930, JAPAN

*E-mail: addisu-bonger-vd@ynu.jp / addbon2@gmail.com

***Abstract*:** There are approximately 20,000 vertical PC steel bars in the Metropolitan Expressway bridges in Japan. In the field survey (in 2018), brittle fracture of vertically tightened PC steel bar was confirmed. One of the main reasons for fracture of PC steel bars was corrosion due to insufficient grout filling. When PC steel bars fractured, all the accumulated strain energy is suddenly released. The PC steel bars protrudes from the anchorage section and damages the covering concrete, which is likely to cause third party damage. In particular, the rupture of vertically-tightened PC steel bars can damage the pavement and may result in car accidents. To prevent these damages, effective and economical protrusion preventing system for vertically tightened PC steel bars are necessary. In this research, after grasping the actual condition of the vertical PC steel bars in the Metropolitan Expressway, numerical simulation of rapture and protrusion of PC steel bars were carried out using Applied Element Method (AEM). The numerical simulations were verified based on the experimental results. In the process of verification, the effects of contact stiffness between elements, material properties, and strain rate were deeply investigated. In addition, numerical simulation investigation was made on the protrusion prevention effects of the pavement on the upper surface of the bridge and of the FRP sheet for concrete spalling prevention on the lower surface of the girder.

Keywords: AEM, prestressed concrete, rupture of vertical PC bars, protrusion of PC bars, concrete spalling

Received: 2019.07.31/ Accepted: 2019.11.13
Internet Journal of Society for Social Management Systems Published Date: 2019.12.20

1. INTRODUCTION

As per April 2017, Metropolitan Expressway (MEX) in Japan had a total length of about 318.9 km. Routes which have been open for 30 years or more comprise about 54.3% of the total length. The proportion of the Metropolitan Expressway occupied by structures such as elevated bridges and tunnels that require detailed maintenance and management is about 95%, which is significantly higher than other roads in other companies. The volume of traffic is as large as 983,000 vehicles/day (average, FY 2016). Traffic volume of large-sized vehicles is about five times that of general roads in Tokyo's 23 wards.

As per 2018 inventory, there are 19,657 vertical PC bars in MEX, where 54.4% of them used in main girder web. About 93% of the vertical PC bars have a length shorter than 3m. Out of 11,435 vertical PC bars, counted from design drawings, about 93% have 15mm to 60mm concrete cover at the bottom surface and around 33.8% have 20mm to 25mm concrete cover on the top surface.

Corrosion of PC bars is seen as a main cause of rupture of PC steel bars.

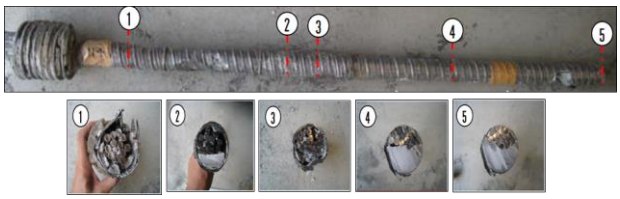

Figure 1: Grouting conditions (Y. Wada et al.)

In the case of rupture of PC strand, wires break one by one and strain energy is released gradually. On the other hand, PC steel bars, since the accumulated strain energy is released all at once, PC steel bars protrudes from the fixing unit and may cause concrete spalling (Central NEXCO, 2009). When the PC bars protruded, the cover concrete is fractured under a high loading rate. It is necessary to consider the effect of strain rate in the numerical simulation.

For plain concrete under high loading rate, the compressive strength, tensile strength & Elastic modulus should increase with an increase in strain rate (P. H. Bischoff and S. H. Perry, 1991, Małgorzata Pająk, 2014, Riisgaard B. et al., 2007). The strain rate effect of concrete under compression and tension at a high loading rate (strain rate > 30/Second) can be calculated using the following equations (Hirotoshi Oo et al., 2006).

$$f'_{cd}/f'_{cs} = \gamma(\dot{\varepsilon}/\dot{\varepsilon}_s)^{1/3}$$
$$f_{td}/f_{ts} = \beta(\dot{\varepsilon}/\dot{\varepsilon}_s)^{1/3}$$

$$\alpha = 1/(5 + 0.9f'_{cs}) \qquad \delta = 1/(10 + 0.6\,f'_{cs})$$
$$\gamma = 10^{(6.156\alpha - 2)} \qquad \beta = 10^{(7.112\delta - 2.33)}$$

Where, f'_{cd}, f_{td} : Compression and tensile strength at rapid loading
f'_{cs}, f_{ts} : Compression and tensile strength at static loading
$\dot{\varepsilon}$: Strain rate at rapid loading
$\dot{\varepsilon}_s$: Strain rate at static loading
(For compressive loading, $30\times10^{-6}[s^{-1}]$,
For tensile loading, $3\times10^{-6}[s^{-1}]$)

Increases in the dynamic modulus, *Ed* expressed as (P. H. Bischoff and S. H. Perry, 1991):

$$E_d/E_s = (\varepsilon_d/\varepsilon_s)^{0.026}$$

Where, E_d : Dynamic modulus,
E_s : Static modulus,
ε_d : Static train rate = $30\text{x}10^{-6}s^{-1}$,
ε_d : Dynamic strain rate

Figure 2: Rupture and protrusion of PC bar (Central NEXCO, 2009)

The objectives of the present study are:

- To evaluate protrusion and concrete spalling prevention performance without considering countermeasure by Applied Element Method (AEM) numerical simulation.
- To verify AEM numerical simulation using experimental results

- To propose sufficient modeling techniques for the upcoming stage of the research.

In 2018, actual rupture of vertical PC bar was investigated by MEX. Type of PC bar was ordinary PC steel bar B type (diameter 32mm and length 2,620mm) (Figure 3). After extracting the PC bar from the sheath, it was confirmed that the bar ruptured at 1345mm from the bottom side and detailed investigation was carried out to study the rupture mechanism. It was concluded that the rupture of PC steel bar was brittle and initiated from corrosion pits which were caused by cyclic drying and wetting due to the ingress of rainy water (Figure 4).

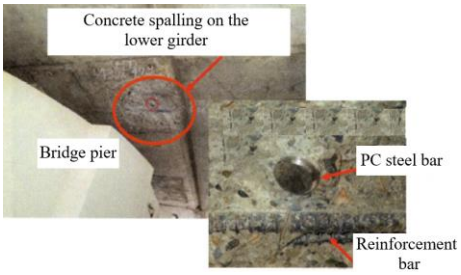

Figure 3: Rupture of vertical PC bar in MEX

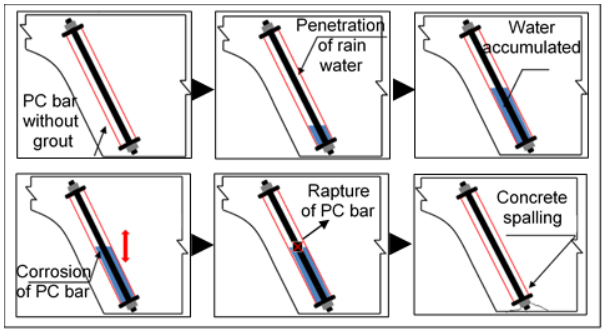

Figure 4: Rupture mechanism of vertical PC bar (Addisu et al., 2019)

2. EXPERIMENTAL PROGRAM

2.1 Specimen details

A reinforced concrete specimen was provided (Figure 5). This specimen had no coupler. PC bar rupture length was 4.5m. Cover concrete was 15mm. Diameter of the sheath was Ø45mm. Grout was not used in the sheath.

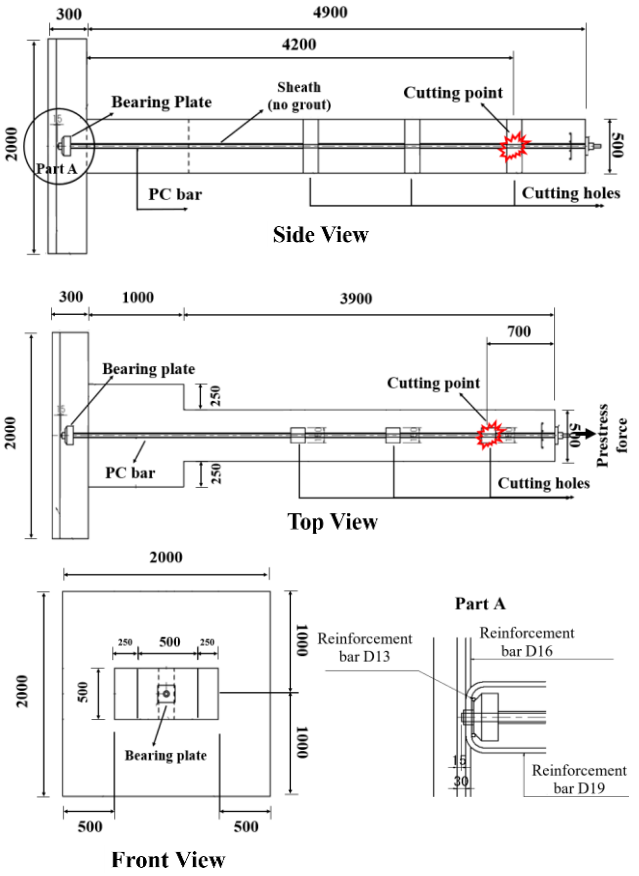

Figure 5: Specimen details

Figure 6: Experiment site condition

2.2 Materials

The concrete had a compressive strength of 40MPa, 8cm slump and 4.5% air volume. The PC bar was Ø32mm, standard steel bar: SBPR930/1180 (class B2). The prestress force was 591 kN (0.6Pu) including prestress loss due to relaxation, creep and shrinkage.

2.3 Testing procedures

The PC bar was inserted into the sheath (Figure 7). Tension force was applied to the PC bar. The PC bar

was cut using grinder at 4.5m from the PC bar head. Then, protrusion of PC bar and concrete spalling were investigated.

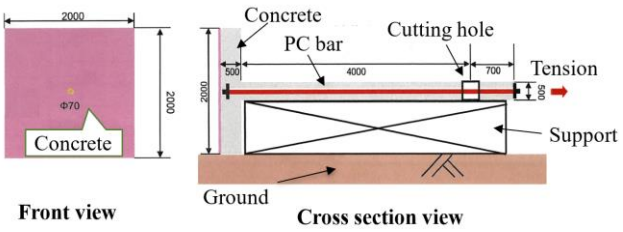

Figure 7: Experiment setup

3. THE APPLIED ELEMENT METHOD (AEM)

In this study, a non-linear structural analysis software `Extreme Loading for Structure (ELS)` based on Applied Element Method (AEM) was used as a nonlinear structural analysis tool to study the behavior of rupture of PC steel bar. AEM allows to perform static or dynamic analysis including cracking, buckling, post-buckling, P-Delta effects, contact, complete element separation, collision, and effects of falling debris. Applied Element Method (AEM) is based on division of the structural members into virtual rigid elements connected through springs. Each spring entirely represents the stresses, strains, deformations, and failure of a certain portion of the structure. The interface material is used to define the springs connecting two rigid bodies with different kinds of material. For modelling concrete under compression, the model of Maekawa including unloading and reloading is adopted (Applied Science International 2017, K. Meguro & H. Tagel-Din 1999, 2000 & 2002).

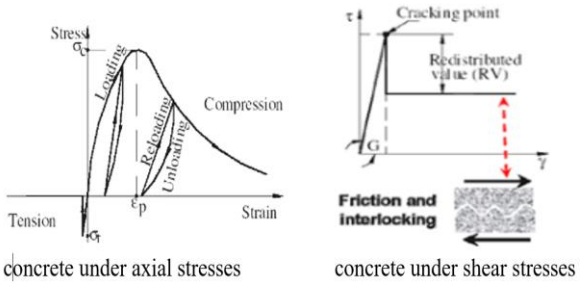

Figure 8: Constitutive models for concrete

The solution for dynamic problems adopts the step-by-step integration (Newmark-beta) method. For nonlinear dynamic phenomenon the numerical solution assumes of a small-time interval that can follow the structural behavior. The time interval required for stable dynamic analysis is a function of element mass and contact stiffness

3.1 Contact Parameters

One of the main break-through features in ELS is automatic element contact detection. Elements may contact and separate, re-contact again or contact other elements without any kind of user intervention. When two elements with different material properties collide, the spring properties are governed by the material with softer properties. When contact occurs between elements, three contact springs are added at each contact point; one normal spring and two shear springs. Those springs are linear springs that transfer energy between elements (Applied Science International, 2017).

a. Normal Contact Stiffness Factor (*NF*)

The normal spring stiffness is calculated as:

Contact spring stiffness = (E)(NF)(D)

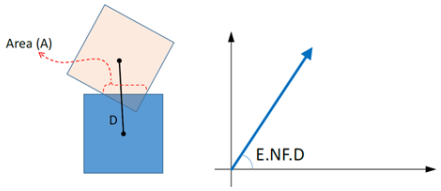

Figure 9: Stiffness value of normal spring when loading occur

b. Shear Contact Stiffness Factor (*SF*)

The shear spring stiffness is affected mainly by friction properties. When shear force is larger than *friction coefficient x normal force*:

Shear spring stiffness = (G)(SF)(D)/1000

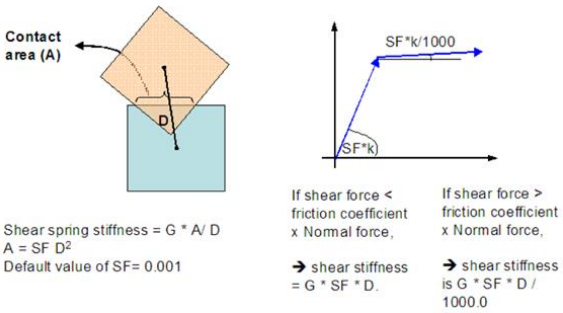

Figure 10: Shear contact stiffness factor

c. Contact Spring Unloading Stiffness Factor *(n)*

When elements collide, some energy is dissipated during contact. Referring to Figure 11, the ratio between loading and unloading stiffness is "*n*".

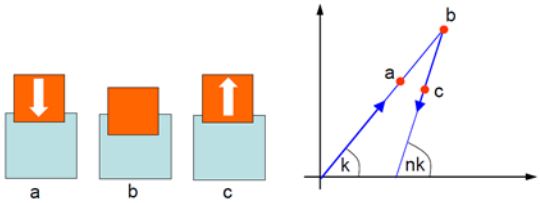

Figure 11: Contact spring unloading stiffness factor

4. ELEMENT CONTACT ANALYSIS

The effects of element contacts were investigated using a simplified model. This simplified model was prepared based on the details showed in Section 2, however the concrete and the reinforcement bars were removed to reduce analysis time (Figure 12). In this case, the bearing plate and the sheath were completely restrained. Rupture length was 4.5m from the PC bar head. The "bearing material" which can transfer only compression was used for the interface between the PC bar and the sheath, and for the interface between the PC bar and the bearing plate. In this analysis two dynamic stages were used. The 1st dynamic stage had a duration of 0.4 second with a time interval of 10^{-5} second and the 2nd dynamic stage had a duration of 0.6 second with a time interval of 10^{-3} second.

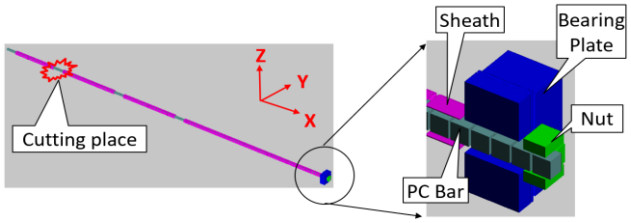

Figure 12: Simplified model to study the effect of element contact

Table 1: Geometry and materials for simplified model

Objects	Geometry		Material
	Cross Section in Y & Z axis (mm)	Length along X axis (mm)	
PC bar	28.36x28.36	5336	High strength steel
Nut	62x62	34	
Bearing Plate	160x160 (40x40 hole)	84	Normal steel
Sheath	40x40	5060	

From parametric study using a simplified model (Figure 12), it was found that the element contact parameters (coefficient of friction, normal contact stiffness factor (NF), Shear contact stiffness factor (SF) and contact spring unloading stiffness factor (n)) had effects on the PC bar protrusion. The following charts showed the effects of element contact on protrusion of PC bar.

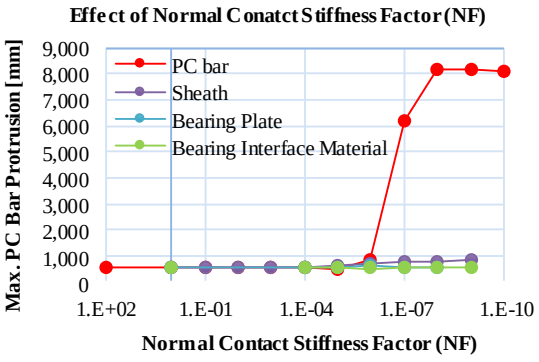

(a)

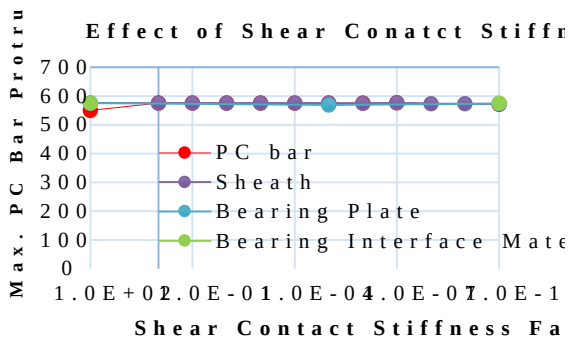

(b)

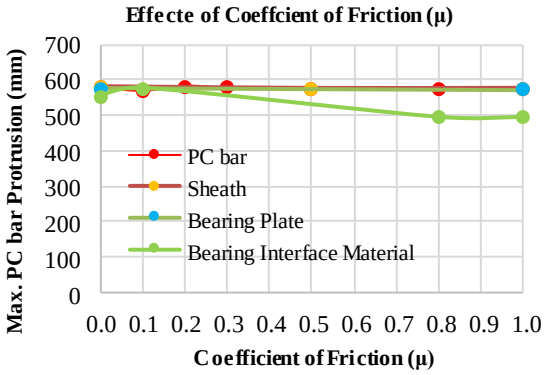

(c)

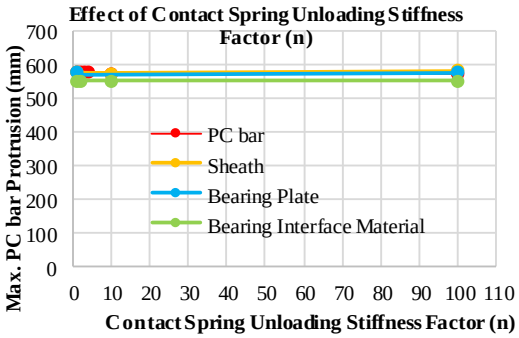

(d)

Figure 13: The effect of element contacts on PC bar protrusion

The investigation indicated that the NF values of the PC bar after 10^{-6} had a significant effect on the protrusion of PC bar. PC bar protrusion increased form 870mm to 6,000mm – 8,000mm for NF values of 10^{-7} – 10^{-10}. However, NF values of the sheath, bearing plate and bearing interface material had small effect on PC bar protrusion.

The effects of SF, μ and n were also investigated for PC bar, sheath, bearing plate and bearing interface material. The analysis results indicated (Figure 13) that SF, μ and n had small effect on PC bar protrusion.

From this parametric study, NF values of the PC bar between 10^{-7} and 10^{-8} gave us a result close to the experiment.

In AEM numerical simulation, actual element contacts between the PC bar and the sheath, the PC bar and the bearing plate and the PC bar and cover concrete were confirmed (Figure 14). The 1st contact between the PC bar and the sheath was generated at 0.034 second after the rupture of the PC bar . After that, the PC bar contacted the sheath and the bearing plate along its length.

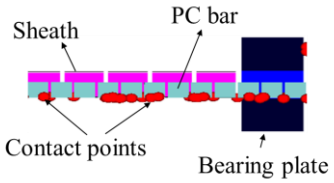

Figure 14: Element contact in AEM simulation

In the experiment, contact between the PC bar and the sheath was also investigated by inserting camera in the sheath at 8 locations (Figure 15(a)). At locations 1 to 4 near to the rupture point, almost no damage in the sheath was observed. As time elapsed, gravity pulls the PC bar down and made more damages on the surface of the sheath at locations 5, 6, 7 and 8. At 5, the PC bar contacted the sheath on the top surface of the sheath but, at 6, 7 and 8 the contact was on the bottom surface of the sheath (Figure 15(b)).

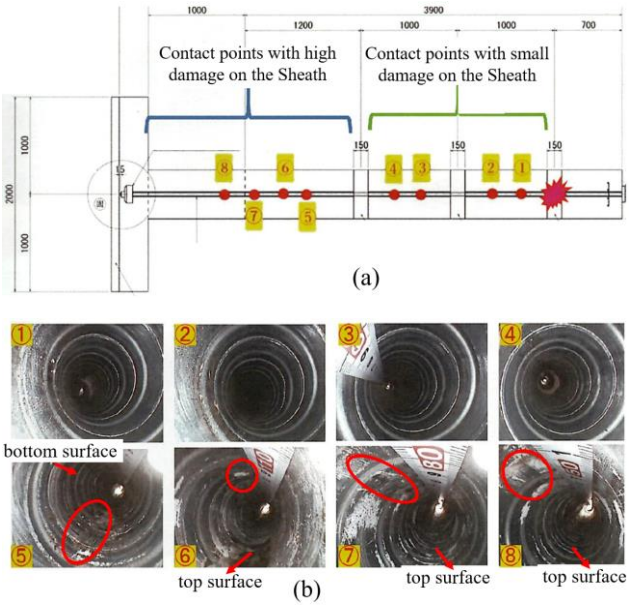

Figure 15: Contact between Sheath and PC bar

5. VERIFICATION AEM NUMERICAL SIMULATION

AEM numerical simulation was made for the experiment explained in section 2.

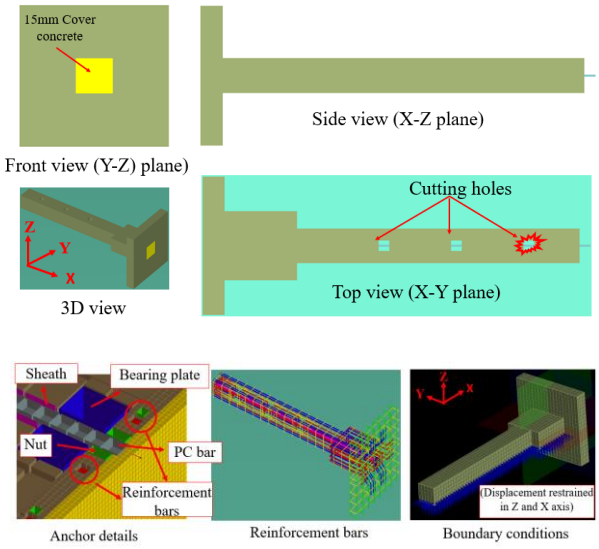

Figure 16: AEM numerical modelling.

Geometry and materials of PC bar, bearing plate, nut and sheath are showed in Table 1. The interface material between (sheath and bearing plate) and PC bar was modelled as a "bearing material". On the other hand, the interface material between (PC bar, nut, bearing plate and sheath) and concrete specimen was modelled as normal concrete (40MPa compressive strength).

In the analysis, three stages of loading were carried out. The first one was static to account for pre-stressing effect, while the second and the third ones were dynamic to simulate the rupture of the PC bar and its impact to the concrete. The 1st dynamic stage had a duration of 0.7 second with a time interval of $5x10^{-6}$ second and the 2nd dynamic stage had a duration of 0.4 second with a time interval of 10^{-3} second. In the dynamic stages, the rupture of the PC bar was simulated by removing one element of the PC bar at the cut point.

5.1 Progressive Failure

Figure 17 shows the protrusion of the PC bar and concrete spalling both in the experiment and in AEM numerical simulation at different time. The protrusion of the PC bar was very fast and energetic. Around 0.4 second after the rupture, the PC bar was fully outside of the sheath. The numerical simulation showed, at 0.584 second, the PC bar made 1st contact with the ground surface (7.104m from the cover concrete). In overall, from 0 – 0.7 second, the AEM numerical simulation showed a good agreement with experiment.

At T = 0.0 Second

At T = 0.05 Second

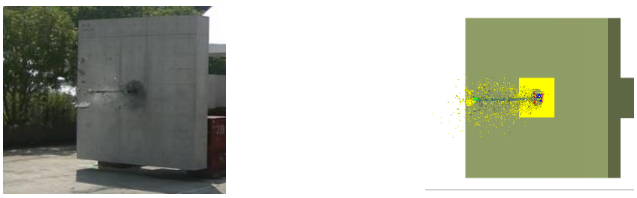

At T = 0.1 Second

At T = 0.2 Second

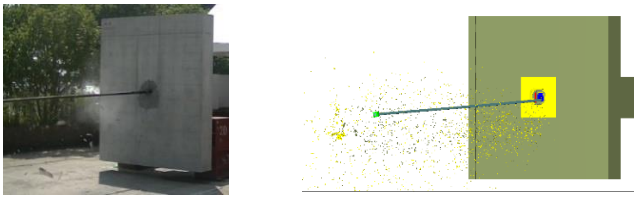

At T = 0.3 Second

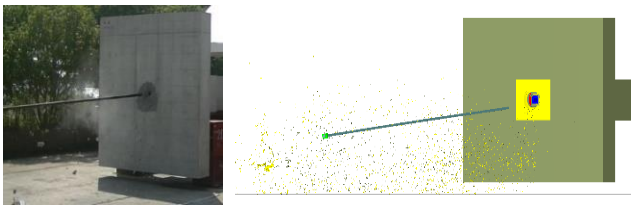

At T = 0.4 Second

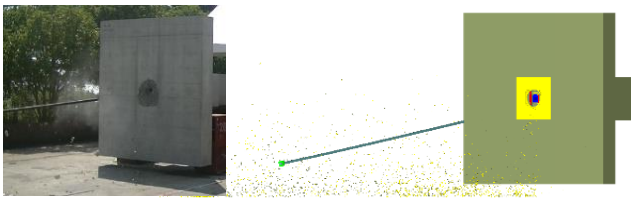

At T = 0.5 Second

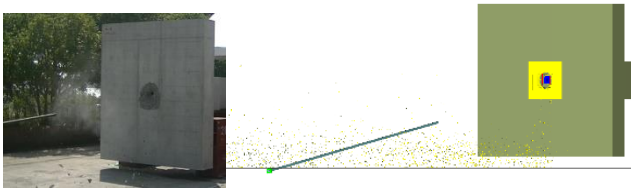

At T = 0.6 Second

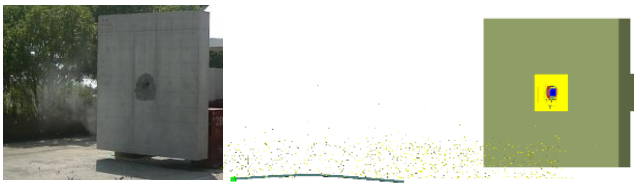

At T = 0.7 Second

Figure 17: Progressive failure Experiment Vs AEM numerical simulation

The PC bar made 1st ground contact at 0.584 Second, 7.104m from the cover concrete. On the other hand, the experiment showed the PC bar made 1st ground contact around 0.6-0.7 second, 7.8m from the cover concrete.

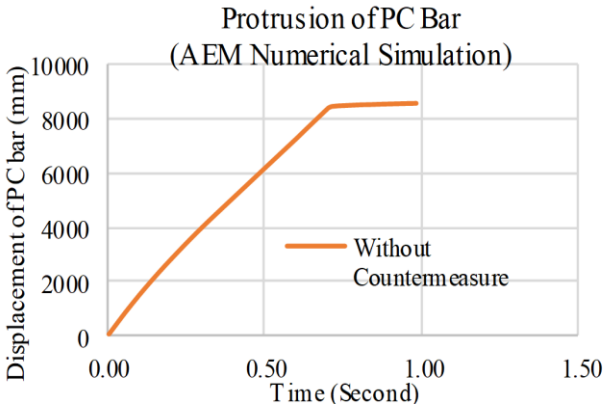

Figure 18: Protrusion of PC bar Vs time

5.2 Concrete Spalling and Failure Mode

The 15mm cover concrete was destroyed and spalled. The cover concrete spalling had a size of around 30cm x 30cm area (Figure 19). The concrete spalling was limited to the centre of the specimen. One of the reasons could be the large amount of reinforcing bars in the cover concrete to prevent specimen failure during prestressing. In numerical simulation, a spalled concrete element with a maximum displacement of 17.721m at 0.98second (18.08m/sec) was found.

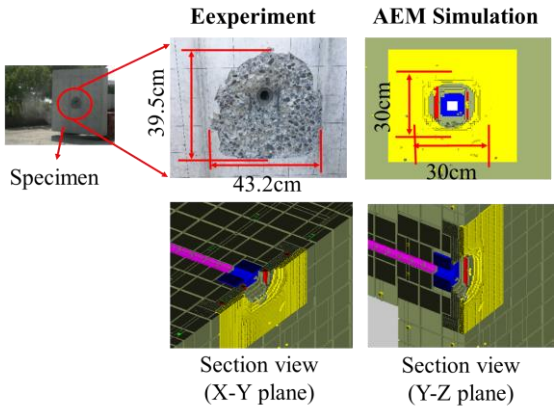

Figure 19: Cover concrete spalling and failure mode

5.3 Surface of ruptured PC bar

The surface of the ruptured PC bar was observed (Figure 20). The cut area of the PC bar by a grinder was 286.4mm^2 which was 35.60% of the PC bar cross section area (804.2mm^2). It took only a few seconds for the grinder to cut the PC bar. The strain energy in the PC bar was strong enough to rupture the PC bar when cut area reached 35.60%. In AEM numerical simulation, cutting of the PC bar was made by removing one element of the PC bar at the cut point and PC bar strain energy lose while cutting was not considered.

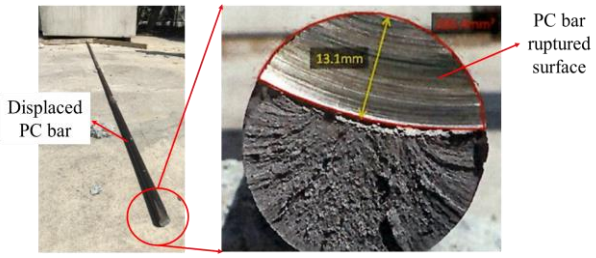

Figure 20: PC bar ruptured surface

5.4 Strain Rate

The normal spring stain rate was checked for the spring between the PC bar and cover concrete and between the nut and cover concrete.

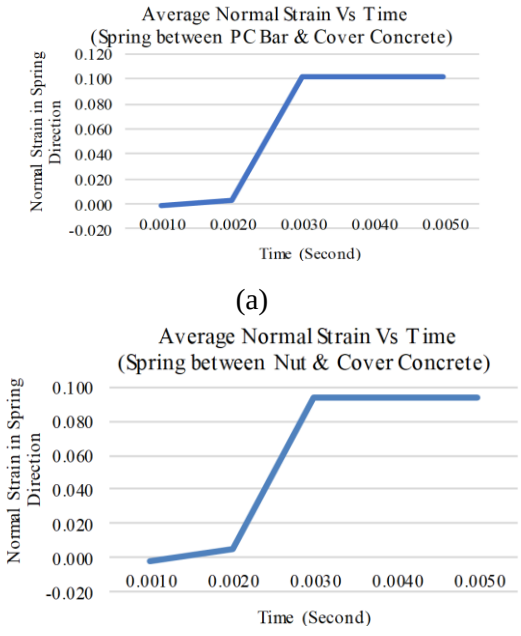

Figure 21: Strain vs time for normal springs

It was found that, the average maximum strain rate for the spring between the nut and cover concrete was 89.7 and the average maximum strain rate for the spring between the PC bar and cover concrete was 97.7. Based on this investigation, rupture of PC bar can be in a high strain rate range of hard impacts (Figure 22).

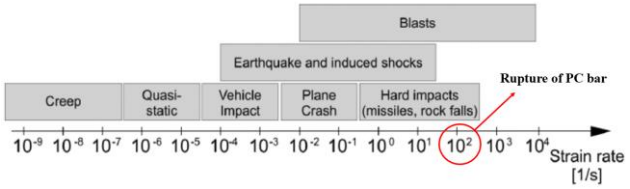

Figure 22: Magnitude of strain rates expected for different loading cases [7]

Therefore, the tensile strength, compressive strength and Young's Modulus of the cover concrete should be increased accordingly. The Dynamic Increase Factors (DIF), the ratio of the dynamic strength to quasi-static strength, are showed in Table 2.

Table 2: The Dynamic Increase Factors

Material Properties	Dynamic Increase Factor (DIF)	
	Springs between PC bar and cover concrete	Springs between nut and cover concrete
Young modulus	1.477	1.474
Tensile strength	2.417	2.350
Compressive strength	2.090	2.031

5.5 Velocity of PC Bar

The velocity of the PC bar was also investigated. The investigation results indicated that the velocity of the PC bar was fluctuating (not constant throughout the dynamic stage (Figure 23). The main reason was the distribution of normal force in the PC

bar was not the same all the time. The direction of normal force in the PC bar was fluctuating towards positive x-axis to negative x-axis (prestressed force direction) and vice versa. When the normal force distribution was towards the positive x-axis, the velocity of the PC bar increased. But, the velocity of the PC bar decreased when the normal force distribution was towards the negative x-axis. For example, Figure 24 showed the normal force distribution of the PC bar at 0.14 second towards positive x-axis and at 0.17 second towards negative x-axis. 0.14 Second and 0.17 Second was randomly chosen to show how the normal force distribution in the PC bar was fluctuating. This could be explained by a dynamic wave transmission along the bar due to sudden loss of its axial force. Around 0.7 second, PC bar velocity drop to zero when the PC bar hits the ground surface.

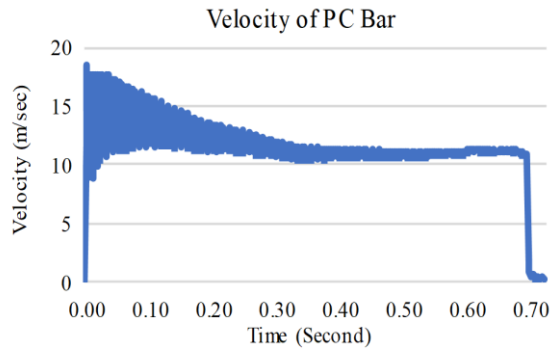

Figure 23: Velocity of PC bar

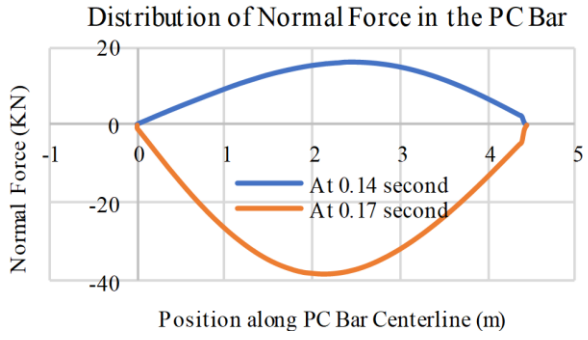

Figure 24: Normal force distribution in the PC bar

6. CONCLUSION

The rupture and protrusion of PC bar from RC specimen was numerically simulated by AEM and verified by the experiment. The followings were obtained.

- Normal contact stiffness factor (*NF*) of the PC bar significantly affected PC bar protrusion. NF values (0.00000005) of PC bar gave us good result.
- 15mm cover concrete was not enough to prevent protrusion of PC bar (32mm diameter and 4.5m rupture length) and concrete spalling. It is recommended to use appropriate countermeasures to prevent protrusion of PC bar and concrete spalling.
- Progressive failure of AEM numerical simulation result showed a good agreement with the Experiment.
- Protrusion of PC bar is a high loading rate and the effect of strain rate should be considered in numerical simulation.

References

1) Addisu Desalegne Bonger, Saeki Fukuhara, Akira Hosoda, Hamed Salem, Takahisa Fukaya and Kazuya Kaba, Rupture and Protrusion of Vertically Tightened PC Bars of PC Bridges, *Proceedings of 11th International Conference of the IFHS on Extreme Engineering*, 2019. (Paper accepted)

2) Applied Science International, URL: http://*Extreme Loading for Structures (ELS)*, 2017.

3) Central NEXCO (Central Nippon Expressway Company Ltd.), *Technical data on Countermeasures for rupture of PC steel bar*, July 2009.

4) Hirotoshi Oo, Koichi Kano, Shinichi Shinai, Takatoshi Sueda, 2006. Comparative analysis of concrete and UFC construction subject to impact load, *Journal of Taisei Corporation*," No. 39.

5) K. Meguro and Hatem Tagel-Din, 1999. Applied Element Simulation for Collapse Analysis of Structures, *Bulletin of Earthquake Resistance Structures*, No. 32

6) K. Meguro and Hatem Tagel-Din, 2000. Applied Element Method for dynamic large deformation analysis of structures, *Structural Eng. / Earthquake Eng., JSCE,* vol. 17, no. 2, pp. 215–224

7) K. Meguro and H. Tagel-din, 2000. Applied Element Method for Structural Analysis, Theory and Application for Linear Materials, *Journal of Doboku Gakkai Ronbunshu*, no. 647, pp. 31–45.

8) K. Meguro and H. Tagel-DIN, 2000. Nonlinear simulation of RC structures using applied element method, *Journal of Doboku Gakkai Ronbunshu*, vol. 17, No. 654, pp. 13–24.

9) K. Meguro, H. Sayed, and T. A. Din, 2002. Applied Element Method Used for Large Displacement Structural Analysis, *Journal of Natural Disaster Science*, vol. 24, No. 1, pp. 25–34,

10) Małgorzata Pająk, 2014. The influence of the strain rate on the strength of concrete taking into account the experimental techniques, *Silesian University of Technology*.

11) P. H. Bischoff and S. H. Perry, 1991. Compressive behavior of concrete at high strain rates, *Materials and Structures / Materiaux et Constructions*, Volume 24, 425-450

12) Riisgaard B., Ngo I. & Mendis P., Georgakis C.T. & Stang H., Dynamic Increase Factors for High Performance Concrete in Compression using Split Hopkinson Pressure Bar, *6th International Conference on Fracture Mechanics of Concrete and Concrete Structures*, Vols 1-3, 2007

13) Yoshinori WADA, Yoshitomi KIMURA, Taku HANAI, "*Study on grout conditions of existing prestressed concrete bridges*".